ACS Sustainable Chemistry & Engineering

Research Article

pubs.acs.org/journal/ascecg

Contribution of Residual Proteins to the Thermomechanical Performance of Cellulosic Nanofibrils Isolated from Green Macroalgae

Jiaqi Guo,[†] Khan Mohammad Ahsan Uddin,[†] Karl Mihhels,[†] Wenwen Fang,[†] Päivi Laaksonen,[†] J. Y. Zhu,[*,†,‡] and Orlando J. Rojas[*,†]

[†]Department of Bioproducts and Biosystems, School of Chemical Engineering, Aalto University, P.O. Box 16300, Espoo 00076, Finland

[‡]Forest Products Laboratory, U.S. Forest Service, U.S. Department of Agriculture, Madison, Wisconsin 53726, United States

Supporting Information

ABSTRACT: Cellulosic nanofibrils (CNFs) were isolated from one of the most widespread freshwater macroalgae, *Aegagropila linnaei*. The algae were first carboxylated with a recyclable dicarboxylic acid, which facilitated deconstruction into CNFs via microfluidization while preserving the protein component. For comparison, cellulosic fibrils were also isolated by chemical treatment of the algae with sodium chlorite. Compared with the energy demanded for deconstruction of wood fibers, algal biomass required substantially lower levels. Nevertheless, the resultant nanofibrils were more crystalline (crystallinity index > 90%) and had a higher degree of polymerization (DP > 2500). Taking advantage of these properties, algal CNFs were used to produce films or nanopapers (tensile strength of up to 120 MPa), the strength of which resulted from protein-enhanced interfibrillar adhesion. Besides being translucent and flexible, the nanopapers displayed unusually high thermal stability (up to 349 °C). Overall, we demonstrate a high-end utilization of a renewable bioresource that is available in large volumes, for example, in the form of algal blooms.

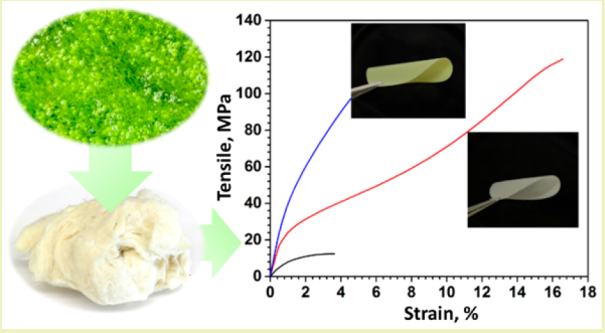

KEYWORDS: *Cellulose nanofibrils, Macroalgae, Nanopaper, Proteins, Thermal stability*

INTRODUCTION

Cellulose nanofibrils (CNFs) have emerged as a biobased material that has captured considerable research and industrial interest. They feature a high aspect ratio, low density, high mechanical strength, and low coefficient of thermal expansion.[1] In addition, they display abundant hydroxyl groups that facilitate CNF functionalization and allow strong interfibrillar hydrogen bonding.[2] The uses of CNFs include those in the fields of biomedical and tissue engineering, bioimaging, nanocomposites, packaging, and functional materials.[3−7] A variety of biomass sources have been used to produce CNFs,[8] which yield characteristic fibril dimensions (length, width), crystallinity, and degree of polymerization.

Among these sources, algae are of special interest despite their relatively low cellulose contents in their native form (20−30%). Indeed, residual streams enriched in cellulose are potentially available in large volumes after the production of advanced biofuels, biochemicals, chlorophyll, and proteins. To this, one can add the fact that algae require short generation cycles and have higher CO_2-sequestering capacity compared with wood; moreover, they are suitable to be grown in culture media, open ponds, wastewater, seawater, brackish water, etc. In addition, algae can be used for marginal land exploitation without interfering with the food chain.[9] Significantly, algal cellulose is known to have high molecular weight and crystallinity,[10,11] ideally suitable for a variety of applications, including polymer reinforcement.

In general, cellulosic nanofibrils are produced by mechanical fibrillation using high-pressure microfluidization, homogenization, or grinding.[12−16] In order to reduce the high energy consumed in direct mechanical fibrillation, chemical and enzymatic pretreatments have been adopted.[17−21] Because algae have a relatively low cellulose content, the severity of any pretreatment in CNF production should be relatively low. In this way one can minimize any loss of yield that results from the removal of noncellulosic components. Mihranyan et al. used sodium chlorite ($NaClO_2$) in an oxidative/bleaching treatment to produce colorless cellulosic material from algae.[11] Although $NaClO_2$ is not an expensive chemical, the addition levels are considerable and may pose environmental pressures. Furthermore, oxidation tends to reduce the crystallinity and thermal stability of cellulose.[22] Recently, Chen and co-workers

Received: April 15, 2017
Revised: June 5, 2017
Published: June 12, 2017

DOI: 10.1021/acssuschemeng.7b01169
ACS Sustainable Chem. Eng. 2017, 5, 6978−6985

proposed recyclable dicarboxylic acids for the partial hydrolysis of wood fibers to yield colloidally stable carboxylated cellulose nanomaterials.[23,24] In the present work, we introduce maleic acid to facilitate CNF production from *Aegagropila linnaei*. Such a system is more attractive not only from the point of view of the environmental impact but also because of the possibility of efficient acid recovery via commercially established crystallization technologies.

Films or "nanopapers" produced from CNFs are attractive green materials that can be used in packaging; they are biodegradable and strong, and besides being flexible and printable, they act as an excellent oxygen barrier.[25,26] Most reports about these materials make use of wood-derived cellulose nanofibrils or lignin-containing CNFs.[27] A recent study indicated that the addition of protein can improve the mechanical properties of related nanocomposites.[28] We have previously discussed the interactions between plant proteins and cellulose.[29−33] Therefore, it is reasonable to assume that the protein naturally present in *Aegagropila linnaei* may be beneficial and an asset for nanopaper production from algae bioresources. Thus, the objective of this study was to understand the advantages of treating green microalgae with a dicarboxylic acid for CNF production. The properties and mechanical performance of nanopapers made from this type of CNFs have been evaluated and compared with those from sodium chlorite treatment, which is known to remove the protein fraction. In turn, this is a stepping stone in the utilization of renewable algae resources (especially relevant to algal bloom management) for value-added applications.[34]

MATERIALS AND METHODS

Materials. Samples of *Aegagropila linnaei*, an algal species widely distributed in the Northern Hemisphere, were harvested from fresh water in The Netherlands. Sodium chlorite ($NaClO_2$, 80%), trichloroacetic acid, Na_2CO_3, NaK tartrate tetrahydrate, $CuSO_4 \cdot 5H_2O$, and maleic acid were purchased from Sigma, Finland. NaOH and HCl (37%) were obtained from VWR, Finland. Lowry reagent was prepared by mixing solutions of 2% (w/v) Na_2CO_3 in 0.1 M NaOH, 1% (w/v) NaK tartrate tetrahydrate, and 0.5% (w/v) $CuSO_4 \cdot 5H_2O$ in a 48:1:1 ratio. The mixture was then incubated at 55 °C for 3 h.

Sugar and Ash Analysis. The carbohydrate content of *Aegagropila linnaei* was determined after a two-step hydrolysis according to a standard method.[35] The ash content was determined gravimetrically via incineration at 575 °C according to ISO 1762 (2001).

Protein Analysis. The protein content of the algae and algal films was determined after a slight modification of the method proposed in ref 9. Briefly, 20 mg of freeze-dried algae was suspended by vortexing in 800 μL of trichloroacetic acid (24% w/v). The suspension was incubated in a water bath at 95 °C for 30 min and diluted 4 times by adding Milli-Q water at room temperature. The suspension was then centrifuged at 13000*g* for 30 min at 4 °C. The supernatant was discarded, and the resultant solid cake was resuspended by vortexing in 2 mL of Lowry reagent. The samples were then centrifuged at 13000*g* for 30 min at room temperature. The supernatant was collected for analysis of the protein content using the Bradford protein assay. The standard curve was prepared using bovine serum albumin as a standard protein in Lowry reagent.

Chemical Pretreatment. Two chemical pretreatment methods, namely, maleic acid hydrolysis (abbreviated as MAH)[23] and $NaClO_2$ oxidation (abbreviated as OX)[11] were used to produce algal CNFs after subsequent mechanical fibrillation.

MAH Method. A 5 g sample of *Aegagropila linnaei* algae was mixed with 100 mL of aqueous solution containing maleic acid (60%). The mixture was heated to 90 °C for 1 h. The solids were then washed with hot water until neutral pH was reached (total yield of 37% based on initial algal mass).

OX Method. A 5.9 g sample of 90% *Aegagropila linnaei* algae was reacted with 2.7 g of $NaClO_2$ in 100 mL of acetate buffer (pH 4.8) at 60 °C for 3 h under mechanical stirring. The solid fraction was washed until neutrality (pH ∼ 7) (solids yield of ∼53%). Never-dried solids (8 g) were then mixed with 100 mL of 0.5 M NaOH solution and kept overnight under stirring at 60 °C. The resultant dispersion was separated and washed with deionized water until neutrality (yield of 42.2%). The never-dried solids were then mixed with 5% HCl and heated until boiling, after which the slurry was allowed to stand overnight. The mass fraction was washed to neutrality again and kept at 4 °C until further use. The overall solids yield based on initial algal mass was 21%.

Mechanical Fibrillation. Maleic acid (0.5%) or hydrolyzed oxidized algal fibers (Figure S1) were homogenized at 30 000 rpm for 3 min (POLYTRON PT 2100, Kinematica AG). The suspensions were then passed once through 400 and 200 μm chambers configured in series at 1500 bar (the obtained samples are hereafter denoted as P0). The P0 samples were further microfluidized using microfluidizer nozzles of smaller diameter (200 and 100 μm used in series) at 2000 bar for a given number of cycles. The CNF samples obtained are hereafter designated with a numeral that indicates the number of passes used (P1, P3, and P5, corresponding to one, three, or five passes). The algal CNFs produced by the MAH and OX methods are denoted as CNF-MAH and CNF-OX, respectively. In the study, the properties of nanofibrils and nanopapers are based on P5 samples.

Nanopapers. Nanopapers were prepared from the two types of CNFs by means of vacuum filtration. A CNF suspension at 2 g/L was stirred overnight, and 6 mL of the suspension was vacuum-filtered using hydrophobic poly(vinyl difluoride) (PVDF) membrane filters with a pore size of 0.22 μm (Durapore GVWP, 0.22 mm, Millipore, USA). The formed wet film was covered with another PVDF membrane and dried at 40 °C overnight.

Characterization. FTIR analyses were carried out using a Nicolet Avatar 360 FTIR spectrometer (Thermo Scientific, USA) in transmittance mode. Dried samples were mixed with KBr to make pellets (ca. 2%). Spectra were acquired for a total of 32 scans in the range 400−4000 cm^{-1} with 4 cm^{-1} resolution. The CNF and respective nanopaper morphologies were determined by scanning electron microscopy (SEM) on a Sigma VP scanning electron microscope (Zeiss , Finland) and atomic force microscopy (AFM) on a multimode atomic force microscope (Bruker, USA). For SEM analyses, CNF samples were prepared by air-drying on silica wafers. Prior to imaging, the samples were sputtered with AuPd for 45 s. For AFM measurements, the nanopapers were fixed on the silica wafer. The characterization was performed in air at 23 °C via AFM with a Nanoscope V controller operated in tapping mode. X-ray diffraction (XRD) measurements were carried out with an X-ray diffractometer (Goniometer Ultima IV, Rigaku Co. Ltd., Japan) equipped with Cu Kα radiation (λ = 0.15406 nm) generated at 45 kV and 40 mA at room temperature. Freeze-dried samples were placed on the sample holder. XRD data were collected at 2θ = 10−40° in steps of 0.013° and were further analyzed using the PANalytical X'Pert HighScore Plus software (Materials Data, Inc.). The apparent degree of crystallinity was calculated using the Segal method.[36]

The molar mass distributions of *Aegagropila linnaei* algae biomass and fibrillated samples (P5) were measured by gel permeation chromatography (GPC) on an Ultimate 3000 system (Dionex, USA) equipped with a refractive index (RI) detector (Shodex RI-101, Shoko Scientific Co., Ltd., Yokohama, Japan). After preactivation by a water/acetone/*N*,*N*-dimethylacetamide (DMAc) solvent exchange sequence, the specimens were dissolved in 90 g/L LiCl/DMAc solution at room temperature. Finally, the LiCl/DMAc solutions were diluted to 9 g/L and filtered through a 0.2 mm syringe filter. The carboxylic acid group content of the CNFs was determined by conductometric titration. The CNF suspensions were protonated by adding an appropriate volume of 1 M HCl (for a final HCl concentration of 0.1 M) and then mixing for 15 min. After protonation, CNF suspensions were dialyzed against Milli-Q water to remove excess protons. Oven-dried CNF material

DOI: 10.1021/acssuschemeng.7b01169
ACS Sustainable Chem. Eng. 2017, 5, 6978−6985

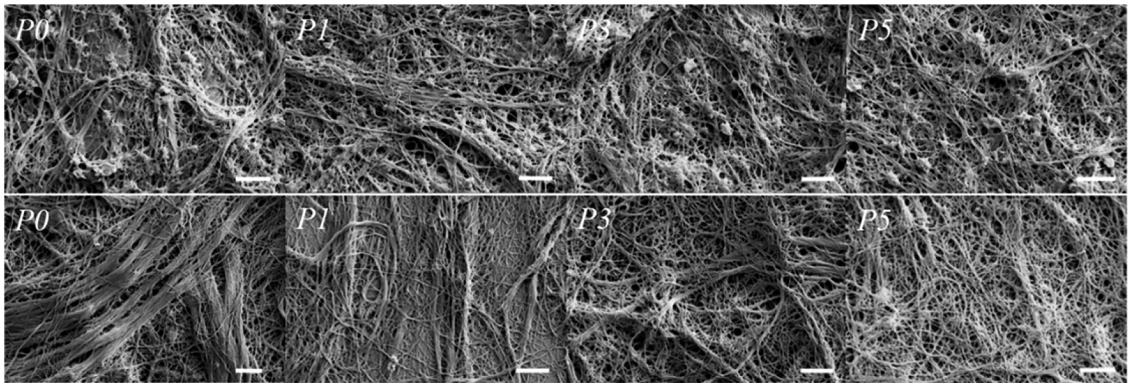

Figure 1. Effects of the extent (number of passes) of microfluidization on the morphologies of two algal CNF samples as revealed by SEM: (top) CNF-MAH; (bottom) CNF-OX. Scale bars = 2 μm.

Table 1. Chemical Composition of *Aegagropila linnaei* Algae

% component					% protein	% ash
glucose	arabinose	rhamonose	galactose	xylose		
33 ± 2	4 ± 0.2	0.45 ± 0.1	5 ± 0.3	0.70 ± 0.5	5.3 ± 0.2	15.7

(100 mg) was dispersed in 200 mL of degassed water, followed by the addition of 0.2 mL of 0.1 M HCl and 0.4 mL of 0.5 M NaCl. The resultant suspension was titrated manually by addition of 40 μL of 0.01 M NaOH every 20 s. The concentration of acid groups was calculated as described in the standard procedure (SCAN-CM 65.02). For each sample, triplicate measurements were conducted, and the average values are reported. The zeta potential of algal CNF suspensions was measured using a Nano ZS90 Instrument. The measurement was carried out at a concentration of 0.2 g/L at pH ~7 and constant electrolyte concentration (5 mM NaCl).

Thermogravimetric analysis (TGA) of the CNF samples was carried out on a Q500 thermogravimetric analyzer (TA Instruments, Germany) using approximately 10 mg of the respective samples. The specimens were dried at 105 °C for 20 min before being heated to 850 °C at a rate of 15 °C/min, and nitrogen was used as the purge gas. The static water contact angles (θ_{st}) of the algal nanopapers were measured using a contact angle meter (CAM 200, KSV Instruments, Ltd., Helsinki, Finland). Images of water droplets (5 μL) placed on the surface of the nanopaper were captured in videos for determination of θ_{st}. Measurements were conducted at three or more different positions on each sample. The mechanical properties of the prepared nanopapers were determined by using 2 mm × 15 mm strips. The specimens were conditioned overnight at 23 °C and 50% relative humidity. Tensile tests were performed with a 5 kN tensile/compression module (Kammrath & Weiss GmbH, Germany) using 100 N load cells (10 mm gauge length and 0.5 mm/min strain rate). Six specimens were measured for each sample, and the average values are reported.

RESULTS AND DISCUSSION

Morphology of Algal CNFs. Elementary fibrils (or microfibrils) from algae are known to be 10−30 nm in width.[37] In this work, the two algal CNF materials (CNF-MAH and CNF-OX) included bundles of cellulosic fibrils that were clearly visible after the first pass through the 200−400 μm chambers connected in series. Compared to the reference CNF-OX (bottom panel of Figure 1), CNF-MAH underwent more extensive fibril deconstruction (top panel of Figure 1). After three passes through the microfluidizer, CNF-MAH fibrils became individualized and homogeneously distributed and displayed what appeared to be protein residues, likely lectins.[38] However, quantitative determination of the protein distribution is very challenging and was not attempted. In principle,

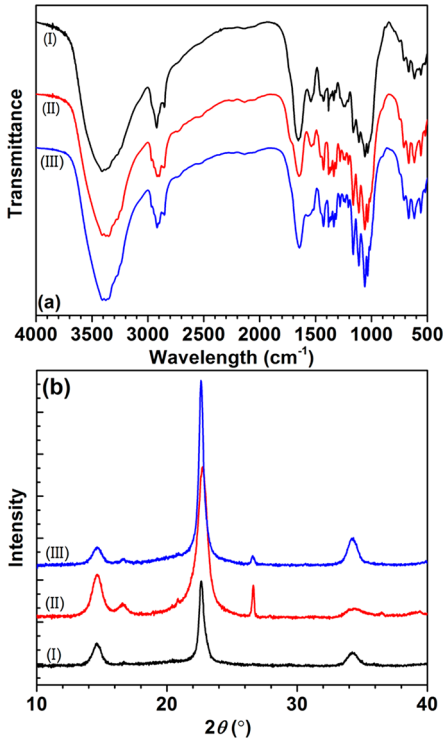

Figure 2. (a) FT-IR and (b) XRD characterization of *Aegagropila linnaei* algae CNF-MAH and CNF-OX. Samples are (I) *Aegagropila linnaei* (raw material), (II) CNF-OX (100:0), and (III) CNF-MAH (93:7).

Table 2. Calculated Crystallinity Indices of Algae (Raw Material), CNF-MAH, and CNF-OX

	crystallinity index (%)	
material	FT-IR	XRD
algae	84	89
CNF-MAH	97	95
CNF-OX	95	94

DOI: 10.1021/acssuschemeng.7b01169
ACS Sustainable Chem. Eng. 2017, 5, 6978−6985

Table 3. Molar Masses of Algal CNFs Compared with Lignocellulosic Nanofibrils (Ligno-CNF)

sample	M_n[a]	M_w[b]	PDI[c]	DP[d]
CNF-MAH	56848	411619	2.7	2540
CNF-OX	80844	590817	4.2	3647
Ligno-CNF[e]	49291	269602	6.3	1664

[a]Number-average molecular weight (g/mol). [b]Weight-average molecular weight (g/mol). [c]Polydispersity index. [d]Degree of polymerization (calculated from M_w using 162 g/mol as the molar mass of the repeat unit). [e]Lignocellulose nanofibrils used as a reference.[43]

microscopic visualization by fluorescent labeling would allow location identification, but the spatial resolution of such a method is at the micrometer level. It can be speculated that the residual proteins were evenly distributed since they were closely connected with the nanofibers. The elevated temperature during the acid treatment most probably led to denaturation and hydrolysis of the proteins. However, this is a question that needs to be addressed given the uncertainties related to the exact type and nature of the residual proteins. Five passes were needed to yield uniform fibrils in CNF-OX. The observations suggested that maleic acid hydrolysis facilitated deconstruction of the algal cell wall by the shear forces applied during fibrillation (fewer passes or less energy consumed to obtain a given fibril size).

Precursor Algae and Algal CNFs. Algae are mainly composed of lipids, proteins, carbohydrates and ash.[9] The composition corresponding to the *Aegagropila linnaei* studied here is shown in Table 1 and Figure S2. The cellulose content of 33 ± 2% was lower than that of wood (typically 40−50%). Moreover, most of the hemicelluloses in this algae species

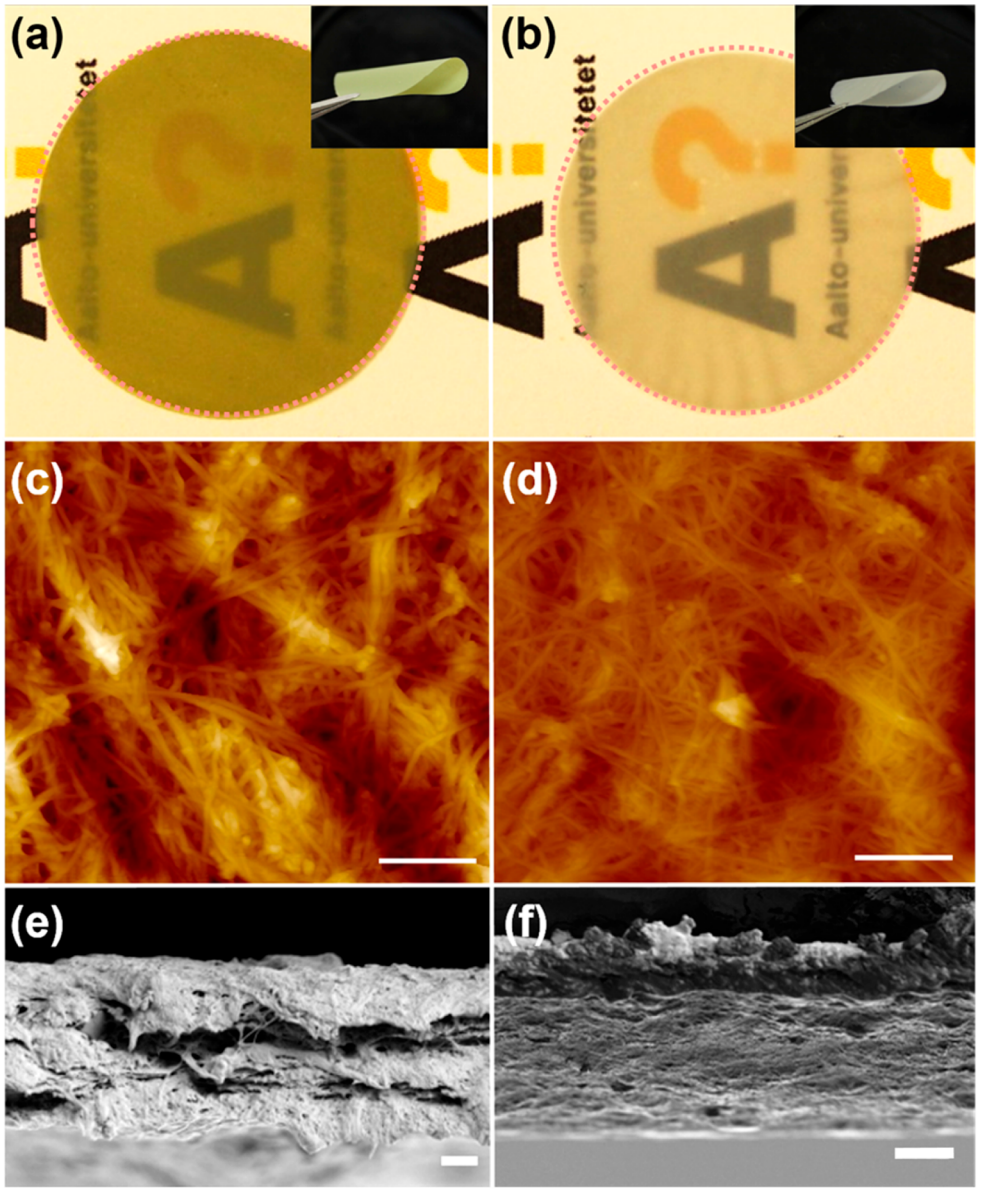

Figure 3. (a, b) Photographs showing translucent (a) NP-OX and (b) NP-MAH algal CNF nanopapers on top of printed characters. The insets show pictures that illustrate the flexibility of the corresponding nanopapers. (c, d) AFM plane-view images of (c) NP-OX and (d) NP-MAH reveal the surface topography of the nanopapers. (e, f) SEM cross-section images of the nanopapers presented in (c) and (d), respectively. Scale bars = 1 μm for both AFM images, 2 μm for the SEM image in (e), and 20 μm for the SEM image in (f).

DOI: 10.1021/acssuschemeng.7b01169
ACS Sustainable Chem. Eng. 2017, 5, 6978−6985

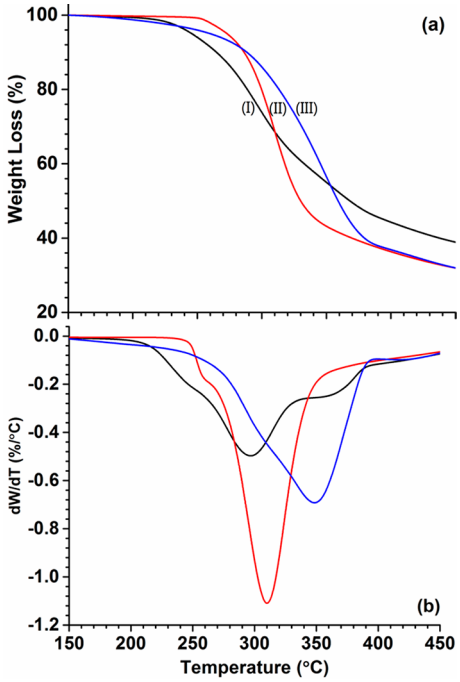

Figure 4. (a) TGA profiles of *Aegagropila linnaei* algae and CNF nanopapers, NP-OX and NP-MAH, to indicate their thermal stability under a nitrogen atmosphere. (b) Temperature first derivative weight loss profiles (dW/dT) of the samples showing the maximum cellulose decomposition. Samples: (I) *Aegagropila linnaei* algae (raw material); (II) CNF-OX (100:0); (III) CNF-MAH (93:7).

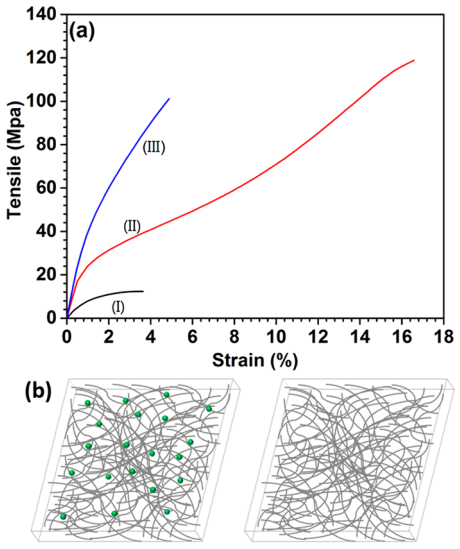

Figure 5. (a) Representative stress−strain profiles for algal nanopapers tested at 50% relative humidity. Samples (cellulose:protein ratios): (I) filter paper; (II) NP-OX (100:0); (III) NP-MAH (93:7). (b) Schematic illustrations of the structures of nanopapers prepared from CNF-MAH (left) and CNF-OX (right). It is expected that NP-MAH is less porous than NP-OX because of the presence of proteins. Compared with NP-OX, NP-MAH contained relatively large amounts of protein residues (cellulose:protein ≈ 93:7), which resulted in improved interfibrillar adhesion and nanopaper strength.

comprised galactose (5 ± 0.3%) and arabinose (4 ± 0.2%). Other minor components included rhamnose (0.45 ± 0.1%) and xylose (0.70 ± 0.5%). The protein content was approximately 5.3 ± 0.2%; a high ash content of 15.7% due to the existence of sand grains and minerals was also determined. FTIR spectra of the algae biomass and the produced CNFs are included in Figure 2a. Both CNF-MAH and CNF-OX displayed prominent bands at 3340, 1170, and 1060 cm^{-1} that were attributed to OH, pyranose ring ether, and C−C groups, respectively. Protein bands in the range of 1500−1660 cm^{-1} were clearly visible.[10]

XRD patterns for CNF-MAH and CNF-OX samples are shown in Figure 2b. Crystallinity index (CrI) values of 95% and 94% were determined, respectively (Table 2). These values were significantly higher than that for the precursor algae material (CrI = 89%), which is explained by the removal of hemicelluloses, disordered cellulose, and impurities from *Aegagropila linnaei* algae after the chemical treatments. On the basis of the electron diffraction results, it has been suggested that the two allomorphs Iα and Iβ coexist. We note the appearance of a peak at $2\theta \sim 27°$ in the case of CNF-OX and CNF-MAH. This has been noted in other reports for products of hydrolysis of microcrystalline cellulose, cellulose nanocrystals, and cellulose nanofibers; however, its origin is not clear.

Oxidation effectively removed the proteins: their concentration was reduced from 5.3 ± 0.2% in the precursor algae to 0.12 ± 0.02% in CNF-OX (CNF:protein = 100:0). Maleic acid hydrolysis was more selective in removing hemicelluloses and resulted in a relatively high residual protein concentration of 6.7 ± 0.2% (CNF:protein = 93:7).

Interestingly, compared with CNF-OX, CNF-MAH had a higher CrI, suggesting that the oxidation in CNF-OX affected the cellulose crystals more strongly. The crystallinity of cellulose was also calculated according to the ratio of the bands at 1372 and 2900 cm^{-1} (H_{1372}/H_{2900}) in the FT-IR spectra.[39] The results were consistent with those determined by XRD (Table 2). The algal CNF crystallinities were much higher than those of CNFs isolated from wood (generally 50−70% depending on the source and measurement method).[37]

Table 3 shows the molar masses of CNF-MAH and CNF-OX (data for ligno-nanocellulose are added as a reference). It is noticed that CNF-MAH had a relatively low polydispersity index, which can be beneficial for certain applications.[40] The two algal CNF materials had higher degrees of polymerization (DP) than the typical wood-derived ligno-nanocellulose.[10,11] The lower DP of CNF-MAH compared with CNF-OX is partially due to the presence of protein (Table 1). The acid hydrolysis also contributed to the reduction in the DP since dicarboxylic acids are known to depolymerize cellulose.[20,41] The acid group contents of CNF-MAH and CNF-OX were 0.44 and 0.14 mmol/g, respectively (Figure S3). The acid groups of CNF-OX corresponded to the acid groups in the original cellulosic fibers, which were relatively few, while the higher acid group content of CNF-MAH was due to the esterification of cellulose with maleic acid,[42] which resulted in cellulose carboxylation.[23,24] The surface charge was determined by measurements of the zeta potential, which corresponded to −32 ± 5 and −9 ± 1 mV for CNF-MAH and CNF-OX, respectively (Figure S4). In summary, compared with CNF-OX, CNF-MAH was more carboxylated and had higher crystallinity and protein content.

Nanopapers. Cellulosic nanofibrils are widely used for the fabrication of films and nanopapers.[44] Nanopapers (NPs) prepared by vacuum filtration from algal CNFs were translucent. Under similar preparation conditions, NP-MAH produced thinner (denser) nanopapers with a thickness of 10

DOI: 10.1021/acssuschemeng.7b01169
ACS Sustainable Chem. Eng. 2017, 5, 6978−6985

Table 4. Comparisons of Ultimate Tensile Stress, Maximum Strain, Specific Strength, Young's Modulus, Specific Modulus, and Toughness of CNF Nanopapers (NPs); Values for TO-CNF and Filter Paper Have Been Added for Comparison

	NP-OX (100:0)	NP-MAH (93:7)	TO-CNF[a]	filter paper
tensile strength (MPa)	109 ± 17	90 ± 7	118.0 ± 12.2	13 ± 2
specific strength (MPa cm^3/g)	111 ± 7	109 ± 21	129.8 ± 6.9	26 ± 5
maximum strain (%)	15 ± 2	4.0 ± 1	0.6 ± 0.1	3.6 ± 0.7
Young's modulus (GPa)	4.5 ± 1	5.8 ± 1	30.3 ± 1.0	1.3 ± 0.3
specific modulus (GPa cm^3/g)	4.6 ± 1	7.1 ± 2	33.4 ± 0.6	2.7 ± 0.7
toughness (J/m^3)	9.2 ± 2.2	2.4 ± 1	N/A	0.34 ± 0.1
yield stress (MPa)	27.4 ± 1.7	44 ± 5.7	N/A	9.7 ± 2.1
thickness (μm)	22.4 ± 0.3	8.5 ± 0.2	35	138 ± 4.9
density (g/cm^3)	0.98	0.83	0.91	0.5

[a]Data for TEMPO-oxidized cellulose nanofibrils from ref 49.

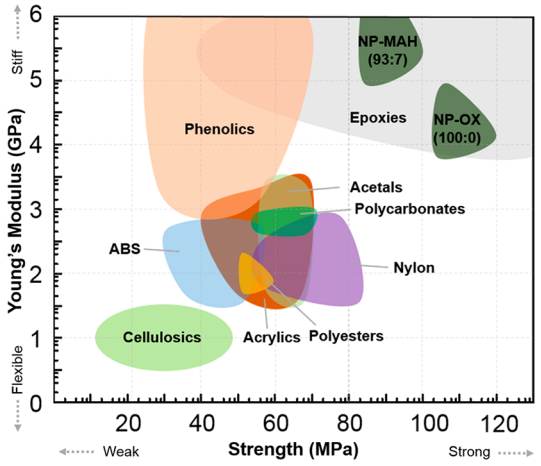

Figure 6. Strength and Young's modulus map to compare nanopapers NP-MAH (93:7) and NP-OX (100:0) against common polymers.

μm, as shown in Figure 3b (those from NP-OX presented a thickness of ca. 25 μm; Figure 3a). This revealed the effect of proteins in densifying the layered structure typical of these films, similar to the effect found for lignin.[45] A printed pattern placed underneath the nanopapers was seen clearly. This can be taken as indicative of the low surface roughness and porosity of the nanopapers.[46] In addition, they were flexible and did not show any sign of cracks or defects upon folding (insets in Figure 3a,b). SEM cross-section images of the nanopapers (Figure 3e,f) indicated that NP-OX nanopapers had a fairly homogeneous, layered structure. In contrast, NP-MAH nanopapers displayed a denser lamellar structure due to the effect of the residual proteins.

The surfaces of the nanopapers were quite smooth, with roughnesses of 104 ± 8 and 101 ± 9 nm for NP-OX and NP-MAH, respectively (Figure 3c,d). The water contact angle (θ_{st}) of NP-MAH was 38 ± 2°, which is higher than that of NP-OX (23.4 ± 1°). This can be attributed to the presence of hydrophobic protein residues (see Figure 5b below for an illustration).

Thermal Stability. TGA thermograms (Figure 4) indicated that the thermal transitions of algae occurred in the range of 150−450 °C and included three phases: (1) moisture evaporation and decomposition of low-molecular-weight saccharides and proteins; (2) decomposition of cellulose; (3) decomposition of residues. Phases (1) and (2) took place below 250 °C.[10] The initial faster weight loss for NP-MAH and the precursor algae was attributed to the presence of proteins. The decomposition of cellulose took place in the range between 250−450 °C. The peak degradation temperatures based on the dW/dT profiles (Figure 4b) were 296, 310, and 349 °C for the algae sample, NP-OX, and NP-MAH, respectively. The increased decomposition temperature for the nanopapers may be attributed to the high crystallinity (Table 2), changes in chemical composition after the respective pretreatment, and other physical and chemical factors.[47,48] NP-MAH had a substantially higher thermal stability (349 °C) compared with that of NP-OX (310 °C), which is partially explained by the higher crystallinity of the former sample; this is consistent with previous work that used oxalic acid.[23]

Mechanical Properties. Tensile tests of both algal CNF nanopapers (NP-MAH and NP-OX) and filter paper (used as a reference) were carried out. The stress−strain profiles for the nanopapers (Figure 5a) indicated that the tensile strength and tensile moduli E of the algal nanopapers were in the range of 90−120 MPa and 4.5−6 GPa, respectively (Table 4). These values were substantially higher than those for filter paper (20 MPa and 1.5 GPa, respectively; Table 4). The maximum strain for NP-OX was remarkably high, ca. 15%, which resulted in a very high toughness of 9.24 MJ/m^3 (Table 4 and Figure 5a). The results were comparable with previous reports (Table S1 and ref 49).

NP-MAH nanopapers, which contained proteins, had a distinctly high yield stress and Young's modulus, both of which were higher than the corresponding values for NP-OX (Table 4). It can be speculated that proteins in NP-MAH filled the voids between the fibrils and increased their interactions and adhesion, resulting in increased stiffness (Figure 5b).[50] Strain hardening in the plastic deformation of NP-OX was observed, which indicated the orientation of fibrils during the deformation.[51] Overall, the mechanical properties of algal nanopapers were comparable to those of commercially available polymeric materials, as indicated in Figure 6 and Table S2. Polymer films were generally very soft and displayed high elongation. The algal nanopapers performed markedly better than the polymer films when considering the combination of toughness, strength, and stiffness.

CONCLUSIONS

Compared with cellulose nanofibrils (CNFs) produced from wood resources, the energy consumed for the deconstruction of green algae to produce CNFs was substantially lower after maleic acid treatment. The CNFs presented high crystallinity (CrI ~ 90%), carboxyl group content (σ > 142 μmol/g), and molecular weight (DP > 2500). The as-produced CNFs were suited for the development of nanopapers, which were translucent and flexible with smooth surfaces and high

DOI: 10.1021/acssuschemeng.7b01169
ACS Sustainable Chem. Eng. 2017, 5, 6978−6985

mechanical strength (tensile strength of 100−120 MPa and maximum strain of 15%). Remarkably, they displayed a significantly high thermal stability (up to 349 °C). Residual proteins were retained after maleic acid hydrolysis, which was beneficial to achieve improved interfibrillar adhesion and strength. Overall, we have demonstrated the use of algae after chemical treatment for potential applications in nanopaper development, which can be relevant to packaging and other areas where films require flexibility, strength, and thermal stability.

■ ASSOCIATED CONTENT

Supporting Information

The Supporting Information is available free of charge on the ACS Publications website at DOI: 10.1021/acssuschemeng.7b01169.

Photograph of algal pulp obtained after OX treatment; HPAEC analysis of *Aegagropila linnaei* in order to determine the sugar content; conductometric titration curves of algal CNF-OX and CNF-MAH; zeta potential values of CNF-MAH and CNF-OX; SEM images of NP-OX and NP-MAH films; summary of NP mechanical properties; and average values of ultimate tensile strength, strain, and Young moduli for common polymers (PDF)

■ AUTHOR INFORMATION

Corresponding Authors

*E-mail: orlando.rojas@aalto.fi.
*E-mail: jzhu@fs.fed.us.

ORCID

Jiaqi Guo: 0000-0001-7557-0356
Päivi Laaksonen: 0000-0003-2029-5275
J. Y. Zhu: 0000-0002-5136-0845
Orlando J. Rojas: 0000-0003-4036-4020

Notes

The authors declare no competing financial interest.

■ ACKNOWLEDGMENTS

This research was supported by the Academy of Finland through the Centres of Excellence Programme (2014−2019). J.Y.Z. acknowledges the J. William Fulbright Foreign Scholarship Board, The Finland−U.S. Education Exchange Commission, and the Finland Fulbright Center for the Fulbright-Aalto University Distinguished Chair Scholarship for his visiting appointment at Aalto University. The authors acknowledge Ms. Ritva Kivelä for technical assistance in algae microfluidization and Dr. Juho Antti Sirviö and Prof. Henrikki Liimatainen (Oulu University, Finland) for material property tests. This work made use of the Aalto University Nanomicroscopy Center (Aalto-NMC) premises.

■ REFERENCES

(1) Klemm, D.; Kramer, F.; Moritz, S.; Lindstrom, T.; Ankerfors, M.; Gray, D.; Dorris, A. Nanocelluloses: A New Family of Nature-Based Materials. *Angew. Chem., Int. Ed.* **2011**, *50*, 5438.

(2) Habibi, Y. Key Advances in the Chemical Modification of Nanocelluloses. *Chem. Soc. Rev.* **2014**, *43*, 1519.

(3) Lin, N.; Dufresne, A. Nanocellulose in Biomedicine: Current Status and Future Prospect. *Eur. Polym. J.* **2014**, *59*, 302−325.

(4) Abdul Khalil, H. P. S.; Bhat, A. H.; Ireana Yusra, A. F. Green Composites from Sustainable Cellulose Nanofibrils: A Review. *Carbohydr. Polym.* **2012**, *87*, 963−979.

(5) Sharma, S.; Zhang, X.; Nair, S. S.; Ragauskas, A.; Zhu, J.; Deng, Y. Thermally Enhanced High Performance Cellulose Nanofibril Barrier Membranes. *RSC Adv.* **2014**, *4*, 45136.

(6) Junka, K.; Guo, J.; Filpponen, I.; Laine, J.; Rojas, O. J. Modification of Cellulose Nanofibrils with Luminescent Carbon Dots. *Biomacromolecules* **2014**, *15*, 876−881.

(7) Huang, J.; Zhu, H.; Chen, Y.; Preston, C.; Rohrbach, K.; Cumings, J.; Hu, L. Highly Transparent and Flexible Nanopaper Transistors. *ACS Nano* **2013**, *7*, 2106−2113.

(8) Sacui, I. A.; Nieuwendaal, R. C.; Burnett, D. J.; Stranick, S. J.; Jorfi, M.; Weder, C.; Foster, E. J.; Olsson, R. T.; Gilman, J. W. Comparison of the Properties of Cellulose Nanocrystals and Cellulose Nanofibrils Isolated from Bacteria, Tunicate, and Wood Processed Using Acid, Enzymatic, Mechanical, and Oxidative Methods. *ACS Appl. Mater. Interfaces* **2014**, *6*, 6127−6138.

(9) Slocombe, S. P.; Ross, M.; Thomas, N.; McNeill, S.; Stanley, M. S. A Rapid and General Method for Measurement of Protein in Micro-Algal Biomass. *Bioresour. Technol.* **2013**, *129*, 51−57.

(10) Xiang, Z.; Gao, W.; Chen, L.; Lan, W.; Zhu, J. Y.; Runge, T. A Comparison of Cellulose Nanofibrils Produced from *Cladophora glomerata* Algae and Bleached Eucalyptus Pulp. *Cellulose* **2016**, *23*, 493.

(11) Mihranyan, A.; Andersson, S. B.; Ek, R. Sorption of Nicotine to Cellulose Powders. *Eur. J. Pharm. Sci.* **2004**, *22*, 279−286.

(12) Abdul Khalil, H. P. S.; Davoudpour, Y.; Islam, M. N.; Mustapha, A.; Sudesh, K.; Dungani, R.; Jawaid, M. Production and Modification of Nanofibrillated Cellulose Using Various Mechanical Processes: A Review. *Carbohydr. Polym.* **2014**, *99*, 649−665.

(13) Hu, C.; Zhao, Y.; Li, K.; Zhu, J. Y.; Gleisner, R. Optimizing Cellulose Fibrillation for the Production of Cellulose Nanofibrils by a Disk Grinder. *Holzforschung* **2015**, *69*, 993−1000.

(14) Qing, Y.; Sabo, R.; Zhu, J. Y.; Agarwal, U.; Cai, Z.; Wu, Y. A Comparative Study of Cellulose Nanofibrils Disintegrated via Multiple Processing Approaches. *Carbohydr. Polym.* **2013**, *97*, 226−234.

(15) Wang, Q. Q.; Zhu, J. Y.; Gleisner, R.; Kuster, T. A.; Baxa, U.; McNeil, S. E. Morphological Development of Cellulose Fibrils of a Bleached Eucalyptus Pulp by Mechanical Fibrillation. *Cellulose* **2012**, *19*, 1631.

(16) Spence, K. L.; Venditti, R. A.; Rojas, O. J.; Habibi, Y.; Pawlak, J. J. A Comparative Study of Energy Consumption and Physical Properties of Microfibrillated Cellulose Produced by Different Processing Methods. *Cellulose* **2011**, *18*, 1097.

(17) Isogai, A.; Saito, T.; Fukuzumi, H. TEMPO-Oxidized Cellulose Nanofibers. *Nanoscale* **2011**, *3*, 71.

(18) Zhu, H.; Luo, W.; Ciesielski, P. N.; Fang, Z.; Zhu, J. Y.; Henriksson, G.; Himmel, M. E.; Hu, L. Wood-Derived Materials for Green Electronics, Biological Devices, and Energy Applications. *Chem. Rev.* **2016**, *116*, 9305−9374.

(19) Henriksson, M.; Henriksson, G.; Berglund, L. A.; Lindström, T. An Environmentally Friendly Method for Enzyme-Assisted Preparation of Microfibrillated Cellulose (MFC) Nanofibers. *Eur. Polym. J.* **2007**, *43*, 3434.

(20) Qin, Y.; Qiu, X.; Zhu, J. Y. Understanding Longitudinal Wood Fiber Ultra-structure for Producing Cellulose Nanofibrils Using Disk Milling with Dilute Acid Prehydrolysis. *Sci. Rep.* **2016**, *6*, 35602.

(21) Wang, W.; Mozuch, M. D.; Sabo, R. C.; Kersten, P.; Zhu, J. Y.; Jin, Y. Production of Cellulose Nanofibrils from Bleached Eucalyptus Fibers by Hyperthermostable Endoglucanase Treatment and Subsequent Microfluidization. *Cellulose* **2015**, *22*, 351.

(22) Fukuzumi, H.; Saito, T.; Okita, Y.; Isogai, A. Thermal Stabilization of TEMPO-Oxidized Cellulose. *Polym. Degrad. Stab.* **2010**, *95*, 1502.

(23) Chen, L.; Zhu, J. Y.; Baez, C.; Kitin, P.; Elder, T. Highly Thermal-Stable and Functional Cellulose Nanocrystals and Nanofibrils Produced Using Fully Recyclable Organic Acids. *Green Chem.* **2016**, *18*, 3835.

DOI: 10.1021/acssuschemeng.7b01169
ACS Sustainable Chem. Eng. 2017, 5, 6978−6985

(24) Bian, H.; Chen, L.; Wang, R.; Zhu, J. Y. Green and Low-Cost Production of Thermally Stable and Carboxylated Cellulose Nanocrystals and Nanofibrils Using Highly Recyclable Dicarboxylic Acids. *J. Visualized Exp.* **2017**, DOI: 10.3791/55079.
(25) Hamedi, M. M.; Hajian, A.; Fall, A. B.; Håkansson, K.; Salajkova, M.; Lundell, F.; Wågberg, L.; Berglund, L. A. Highly Conducting, Strong Nanocomposites Based on Nanocellulose-Assisted Aqueous Dispersions of Single-Wall Carbon Nanotubes. *ACS Nano* **2014**, *8*, 2467−2476.
(26) Koga, H.; Saito, T.; Kitaoka, T.; Nogi, M.; Suganuma, K.; Isogai, A. Transparent, Conductive, and Printable Composites Consisting of TEMPO-Oxidized Nanocellulose and Carbon Nanotube. *Biomacromolecules* **2013**, *14*, 1160−1165.
(27) Zhu, H.; Zhu, S.; Jia, Z.; Parvinian, S.; Li, Y.; Vaaland, O.; Hu, L.; Li, T. Anomalous Scaling Law of Strength and Toughness of Cellulose Nanopaper. *Proc. Natl. Acad. Sci. U. S. A.* **2015**, *112*, 8971.
(28) Arboleda, J. C.; Hughes, M.; Lucia, L. A.; Laine, J.; Ekman, K.; Rojas, O. J. Soy Protein-Nanocellulose Composite Aerogels. *Cellulose* **2013**, *20*, 2417.
(29) Salas, C.; Rojas, O. J.; Lucia, L. A.; Hubbe, M. A.; Genzer, J. Adsorption of glycinin and β-conglycinin on silica and cellulose: surface interactions as a function of denaturation, pH, and electrolytes. *Biomacromolecules* **2012**, *13*, 387−396.
(30) Fritz, C.; Jeuck, B.; Salas, C.; Gonzalez, R.; Jameel, H.; Rojas, O. J. Nanocellulose and Proteins: Exploiting Their Interactions for Production, Immobilization, and Synthesis of Biocompatible Materials. *Adv. Polym. Sci.* **2015**, *271*, 207−224.
(31) Langdon, B. B.; Mirhossaini, R. B.; Mabry, J. N.; Sriram, I.; Lajmi, A.; Zhang, Y.; Rojas, O. J.; Schwartz, D. K. Single-molecule resolution of protein dynamics on polymeric membrane surfaces: The roles of spatial and population heterogeneity. *ACS Appl. Mater. Interfaces* **2015**, *7*, 3607−3617.
(32) Arboleda, J. C.; Niemi, N.; Kumpunen, J.; Lucia, L. A.; Rojas, O. J. Soy protein-based polyelectrolyte complexes as biobased wood fiber dry strength agents. *ACS Sustainable Chem. Eng.* **2014**, *2*, 2267−2274.
(33) Khakalo, A.; Filpponen, I.; Johansson, L.; Vishtal, A.; Lokanathan, A. R.; Rojas, O. J.; Laine, J. Using gelatin protein to facilitate paper thermoformability. *React. Funct. Polym.* **2014**, *85*, 175−184.
(34) Mihranyan, A. Cellulose from Cladophorales Green Algae: From Environmental Problem to High-Tech Composite Materials. *J. Appl. Polym. Sci.* **2011**, *119*, 2449.
(35) Sluiter, A.; Hames, B.; Ruiz, R.; Scarlata, C.; Sluiter, J.; Templeton, D.; Crocker, D. Determination of Structural Carbohydrates and Lignin in Biomass Laboratory Analytical Procedure (LAP). NREL Technical Report 2011, NREL/TP-510-42618 (version 07−08−2011).
(36) Segal, L.; Creely, J. J.; Martin, A. E.; Conrad, C. M. An Empirical Method for Estimating the Degree of Crystallinity of Native Cellulose Using the X-Ray Diffractometer. *Text. Res. J.* **1959**, *29*, 786−794.
(37) Le Bras, D.; Strømme, M.; Mihranyan, A. Characterization of Dielectric Properties of Nanocellulose from Wood and Algae for Electrical Insulator Applications. *J. Phys. Chem. B* **2015**, *119*, 5911−5917.
(38) Teixeira, E. H.; Arruda, F. V. S.; do Nascimento, K. S.; Carneiro, V. A.; Nagano, C. S.; da Silva, B. R.; Sampaio, A. H.; Cavada, B. S. In *Carbohydrates—Comprehensive Studies on Glycobiology and Glycotechnology*; Chang, C. F., Ed.; InTech: Rijeka, Croatia, 2012; pp 533−558.
(39) Nelson, M. L.; O'Connor, R. T. Relation of Certain Infrared Bands to Cellulose Crystallinity and Crystal Lattice Type. Part II. A New Infrared Ratio for Estimation of Crystallinity in Celluloses I and II. *J. Appl. Polym. Sci.* **1964**, *8*, 1325−1341.
(40) Dai, C. A.; Yen, W. C.; Lee, Y. H.; Ho, C. C.; Su, W. F. Facile Synthesis of Well-Defined Block Copolymers Containing Regioregular Poly(3-hexyl thiophene) via Anionic Macroinitiation Method and Their Self-Assembly Behavior. *J. Am. Chem. Soc.* **2007**, *129*, 11036−11038.
(41) Wang, R.; Chen, L.; Zhu, J.; Yang, R. Tailored and integrated production of carboxylated cellulose nanocrystals (CNC) with nanofibrils (CNF) through maleic acid hydrolysis. *ChemNanoMat* **2017**, *3*, 328.
(42) Fischer, E.; Speier, A. Darstellung der Ester. *Ber. Dtsch. Chem. Ges.* **1895**, *28*, 3252−3258.
(43) Guo, J.; Filpponen, I.; Su, P.; Laine, J.; Rojas, O. J. Attachment of gold nanoparticles on cellulose nanofibrils via click reactions and electrostatic interactions. *Cellulose* **2016**, *23*, 3065.
(44) Guo, J.; Fang, W.; Welle, A.; Feng, W.; Filpponen, I.; Rojas, O. J.; Levkin, P. A. Superhydrophobic and Slippery Lubricant-Infused Flexible Transparent Nanocellulose Films by Photoinduced Thiol−Ene Functionalization. *ACS Appl. Mater. Interfaces* **2016**, *8*, 34115−34122.
(45) Rojo, E.; Peresin, M. S.; Sampson, W. W.; Hoeger, I. C.; Vartiainen, J.; Laine, J.; Rojas, O. J. Comprehensive elucidation of the effect of residual lignin on the physical, barrier, mechanical and surface properties of nanocellulose films. *Green Chem.* **2015**, *17*, 1853.
(46) Xu, X.; Zhou, J.; Jiang, L.; Lubineau, G.; Ng, T.; Ooi, B. S.; Liao, H. Y.; Shen, C.; Chen, L.; Zhu, J. Y. Highly Transparent, Low-haze, Hybrid Cellulose Nanopaper as Electrodes for Flexible Electronics. *Nanoscale* **2016**, *8*, 12294.
(47) Kargarzadeh, H.; Ahmad, I.; Abdullah, I.; Dufresne, A.; Zainudin, S. Y.; Sheltami, R. M. Effects of hydrolysis conditions on the morphology, crystallinity, and thermal stability of cellulose nanocrystals extracted from kenaf bast fibers. *Cellulose* **2012**, *19*, 855.
(48) Huang, F. Thermal properties and thermal degradation of cellulose tri-stearate (CTs). *Polymers* **2012**, *4*, 1012.
(49) Sirviö, J. A.; Kolehmainen, A.; Visanko, M.; Liimatainen, H.; Niinimäki, J.; Hormi, O. E. Strong, Self-Standing Oxygen Barrier Films from Nanocelluloses Modified with Regioselective Oxidative Treatments. *ACS Appl. Mater. Interfaces* **2014**, *6*, 14384−14390.
(50) Malho, J.; Ouellet-Plamondon, C.; Rüggeberg, M.; Laaksonen, P.; Ikkala, O.; Burgert, I.; Linder, M. B. Enhanced plastic deformations of nanofibrillated cellulose film by adsorbed moisture and protein-mediated interactions. *Biomacromolecules* **2015**, *16*, 311−318.
(51) Malho, J.; Arola, S.; Laaksonen, P.; Szilvay, G. R.; Ikkala, O.; Linder, M. B. Modular Architecture of Protein Binding Units for Designing Properties of Cellulose Nanomaterials. *Angew. Chem., Int. Ed.* **2015**, *54*, 12025.

DOI: 10.1021/acssuschemeng.7b01169
ACS Sustainable Chem. Eng. 2017, 5, 6978−6985